Proceedings of the Twenty-sixth (2016) International Ocean and Polar Engineering Conference **www.isope.org**
Rhodes, Greece, June 26-July 1, 2016

ISBN 978-1-880653-88-3; ISSN 1098-6189

A Hybrid Heading Control Scheme for a Biomimetic Underwater Vehicle

Rui Wang, Shuo Wang, Yu Wang
State Key Laboratory of Management and Control for Complex Systems,
Institute of Automation, Chinese Academy of Sciences
Beijing, China

ABSTRACT

This paper addresses the novel design of a biomimetic underwater vehicle (BUV) propelled by undulatory fins and its heading control problems. Inspired by the cuttlefish, which can perform flexible motions by undulatory propulsion in narrow spaces, our BUV with two undulatory fins is designed. The specific implementation of mechanical structure is elaborated. Moreover, a hybrid heading control which combines active disturbance rejection control (ADRC) with fuzzy strategy is proposed to achieve accurate heading control for this BUV. In the end, experimental results demonstrate the feasibility and effectiveness of the mechanism and control system.

KEY WORDS: Biomimetic underwater vehicle; undulatory fin; heading control; active disturbance rejection control; fuzzy inference.

INTRODUCTION

Various autonomous underwater vehicles (AUVs) have been developed as ocean industries have grown rapidly (Blidberg, 2001; Ayutthaya, Tiaple, Laitongdee and Iamraksa, 2014). Nevertheless, operations in dangerous and worse environments are more complicated. To address increasing demands for high mobility, robustness and improved disturbance rejection, many researchers and engineers have attempted to design biomimetic AUVs. (Chu, Lee, Song, Han, Lee, Kim, Kim, Park, Cho and Ahn, 2012).

Recently, many BUVs propelled by undulatory fins have been built (Curet, Patankar, Lauder and MacIver, 2011; Hu, Low, Shen and Xu, 2012; Zhou and Low 2012; Rahman, Sugimori, Miki, Yamamoto, Sanada and Toda, 2013). However, most of researchers focus on undulatory fin control, but seldom consider precise heading control for those BUVs in underwater missions.

Heading control is a vital issue for the successful operation of a BUV. Although prior researchers have achieved satisfactory performance (Perez, 2006; Yu, Bao and Nonami, 2008), most heading controllers only aim to obtain the course stabilization of ships by steering the rudder angle, which is quite different from that of BUVs by coordinating the fins. Few researchers have presented some effective approaches to deal with heading control for BUVs (Wei, Wang, Wang, Zhou and Tan, 2015). They proposed a course controller to make a BUV rotate to a given angle in situ, while it's more helpful to control the heading of BUVs at a certain swimming speed.

In this paper, we design a novel BUV propelled by undulatory fins and present an effective solution to heading control for the BUV. The main contributions of this paper are summarized as follows.

1) An improved BUV named RobCutt-II, based on our previous design (Wei, Wang, Wang, Zhou and Tan, 2015) is presented. RobCutt-II contains an underwater manipulator system (Wang, Wang, Wei and Tan, 2015). Two biomimetic underwater propulsors (Wang and Wang, 2015) are mounted on both sides of the manipulator system symmetrically. Each propulsor consists of a cylindrical cavity and an undulating long fin. With the coordinated control of the propagating waves on bilateral fins, RobCutt-II can perform many motions, including forward/backward swimming, diving/floating motion, and turning maneuver with high mobility.
2) Heading control of RobCutt-II is designed in order to maintain the desired heading angle when RobCutt-II swims. The basic concept of this control method is to use active disturbance rejection control technique (Han, 2009) for total disturbance estimation.
3) Fuzzy logic model (Klir and Yuan, 1995) is proposed to build the nonlinear relationship between force/torque and the control inputs of RobCutt-II, i.e., the parameters of propagating waves on bilateral fins including the left fin frequency, the right fin frequency, amplitude of waves and the phase difference. Therefore, the hybrid control scheme combining ADRC with fuzzy strategy can be used to precisely control the heading of the RobCutt-II in underwater missions.

In the remainder of this paper, the mechanism design and system configuration of the RobCutt-II are described in Section II. Hybrid heading control scheme which combines ADRC with fuzzy strategy is elaborated in Section III. Experimental results are further provided in Section IV. Finally, the conclusion is presented in Section V.

DESIGN OF BUV ROBCUTT-II

Cuttlefish are marine animals swimming by undulations of a pair of lateral fins. They can perform flexible motions in narrow spaces with water turbulence. Motivated by this unique propulsion mode, our biomimetic underwater vehicle-RobCutt-II is designed.

Mechanism design of the RobCutt-II

The mechanism design for the RobCutt-II is based on modular concepts. As shown in Fig. 1, the RobCutt-II can be divided into three parts, i.e., main body, a five degrees of freedom manipulator and modular propulsors with undulatory fins. Servo motors for driving the manipulator, controller, sensors and their batteries are installed inside the main body. Furthermore, those servo motors are connected to the joints of the manipulator by timing belt pulley, gear or wire rope transmission. This concept design reduces the coupling between the manipulator and the vehicle, which are conductive to high-speed underwater operation (Wang, Wang, Wei and Tan, 2015).

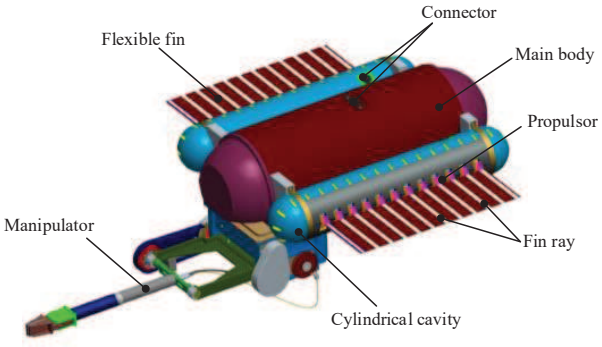

Fig. 1 Mechanical design of the RobCutt-II

Fig. 2 shows that the propulsor also contains two sub-modules: cylindrical cavity and long fin. The mechanism reduces the motion resistance in the underwater space. Driving board, batteries and servo motors for driving the long fin are integrated inside the cylindrical cavity. The long fin consists of twelve fin rays which are connected to one another by a flexible membrane made of thin rubber isometrically. Each fin ray can be independently controlled by the corresponding servo motor. In particular, owing to the modular design, the propulsor module can swim in the water independently or be used to construct various biomimetic robots of fish swimming by fin undulations.

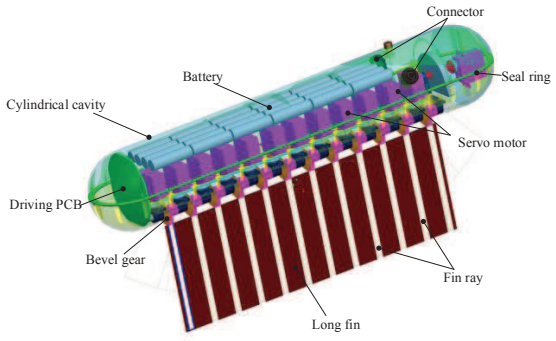

Fig. 2 Implementation of propulsor with a undulating fin

As demonstrated in Fig. 3, two aforementioned propulsors are mounted on both sides of the underwater manipulator system symmetrically by screws and iron hoops and the prototype RobCutt-II is fabricated. Table I tabulates the main structure parameters of the RobCutt-II prototype. Since the buoyancy is slightly larger than the gravity, the RobCutt-II will float in the water when it is at rest. Moreover, benefiting from the bilateral symmetrical structure and large metacentric height, the RobCutt-II has good static stability of roll and pitch angles.

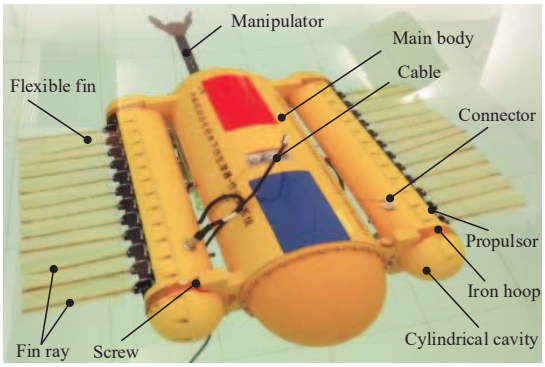

Fig. 3 RobCutt-II prototype

Table 1 Structure parameters of the RobCutt-II prototype

Parameters	value	Parameters	value
Mass	51.9 kg	Weight	508.62 N
Buoyancy	510.58 N	Main body length	760.6 mm
Main body diameter	260 mm	Cavity length	665 mm
Cavity diameter	120 mm	Fin length	460 mm
Fin width	165 mm	Fin thickness	0.82 mm
Number of fin rays	12	Space of fin rays	43 mm
Frequency	0-2.5 Hz	Amplitude	10° – 40°
Number of waves	0 – 2	Deflection angle	−50° – 50°

System Configuration of the RobCutt-II

The system configuration for the vehicle consists of decision control unit and driving unit as shown in Fig. 4.

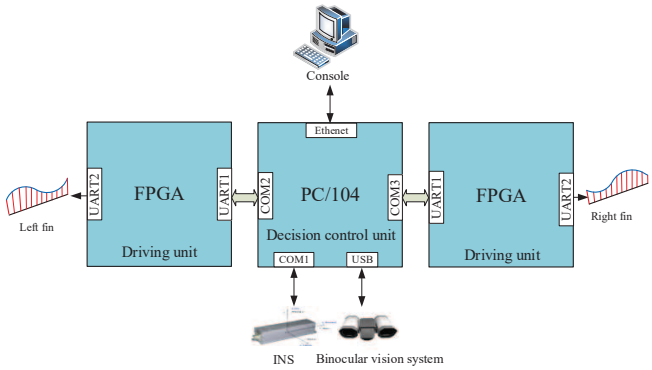

Fig. 4 System configuration of the RobCutt-II

The decision control unit employs a PC/104 module (Advantech 3363D) as the master chip mainly to collect and process sensor data and then analyze the control command. Along with the PC/104 module, inertial navigation system (INS) and a binocular vision system for collecting

the visual information behind vehicle are attached to the interior of the RobCutt-II. Moreover, the decision control unit is connected to remote console via a cable. In this way, the console can control the movement of the RobCutt-II manually.

The driving unit is based on embedded control system. A Field Programmable Gate Arrays (FPGA) chips (ALTERA EP3C55F484) is used to control the undulatory fin. The driving unit is in charge of receiving the commands from the decision control unit, parsing out motion parameters, i.e., frequency, amplitude and phase of the propagating waves on long fins, and finally sending corresponding commands to servo motors under the specific communication protocol.

With the coordinated control of the propagating waves on bilateral fins, RobCutt-II can perform different swimming modes, including forward/backward swimming, diving/floating motion, and turning maneuver with high mobility.

HYBRID HEADING CONTROLLER DESIGN

This section presents the algorithm of hybrid controller to solve the aforementioned heading control problem of the RobCutt-II. The model of the RobCutt-II is firstly proposed in this section. Then the hybrid heading control scheme which combines ADRC with fuzzy strategy is presented. Finally, the algorithms are presented in detail respectively in the rest of this section.

Model of the RobCutt-II

As previously described, the RobCutt-II has good static stability due to large metacentric height, so it's reasonable to neglect the motion in pitch and roll. Furthermore, we assume that the motion in surge and heave are decoupled from the motion in sway and yaw. Therefore, it's sufficient to consider only the 3 degrees-of-freedom when designing heading controller for the RobCutt-II . The 3 DOF kinematic and dynamics can be represented as (Fossen, 2002):

$$\begin{aligned} &\dot{\eta} = J(\psi)\nu \\ &M\dot{\nu} = -C(\nu)\nu - D\nu + \tau + \tau_d \end{aligned} \tag{1}$$

where $\eta = [x, y, \psi]^T \in \mathbb{R}^3$ represents the earth-fixed position and heading, $J(\psi) \in SO(3)$ is the rotation matrix from the earth-fixed local geographic reference frame to the vehicle-fixed reference frame, $\nu = [u, v, r]^T \in \mathbb{R}^3$ represents the body-fixed velocities, M is the vehicle inertia matrix, $C(\nu)$ is the centrifugal and coriolis matrix, D is the hydrodynamic damping matrix, $\tau = [\tau_u, 0, \tau_r]^T \in \mathbb{R}^3$ represents the vehicle-fixed propulsion force and moment, and $\tau_d = [\tau_{du}, \tau_{dv}, \tau_{dr}]^T \in \mathbb{R}^3$ describes the disturbance forces or moment acting on surge, sway and yaw. In particular, the matrixes M and D are assumed to have the following structure based on the foregoing decoupling assumption:

$$M \triangleq \begin{bmatrix} m_{11} & 0 & 0 \\ 0 & m_{22} & 0 \\ 0 & 0 & m_{33} \end{bmatrix}, D \triangleq \begin{bmatrix} d_{11} & 0 & 0 \\ 0 & d_{22} & 0 \\ 0 & 0 & d_{33} \end{bmatrix} \tag{2}$$

With the particular structure of the inertia matrix M given in Eq. (2), the centripetal and coriolis matrix $C(\nu)$ is parameterized as in Eq. (3).

$$C(\nu) \triangleq \begin{bmatrix} 0 & 0 & -m_{22}v \\ 0 & 0 & m_{11}u \\ m_{22}v & -m_{11}u & 0 \end{bmatrix} \tag{3}$$

Finally, the dynamic equation of heading can be rewritten as

$$\begin{aligned} &\dot{\psi} = r \\ &\dot{r} = f_r + b_r\tau_r \end{aligned} \tag{4}$$

where $f_r = \frac{m_{11}-m_{22}}{m_{33}}uv - \frac{d_{33}}{m_{33}}r + \frac{1}{m_{33}}\tau_{dr}$ is a multivariable function of system states, external disturbances and time; $b_r = \frac{1}{m_{33}}$ denotes the control gain.

Hybrid heading control scheme

Heading control is essential for a practical BUV to complete tasks. However, BUV with two undulatory fins is a multi-variable, nonlinear and strong-coupling system, which is difficult to develop precise mathematical model. Aforementioned model is a rough model with large model uncertainties due to the assumption of decoupling and symmetry. Therefore, a hybrid control combining ADRC with fuzzy strategy is designed to achieve closed-loop heading control for the RobCutt-II and the block diagram is illustrated in Fig. 5. The hybrid heading controller is mainly composed of two components, i.e., ADRC controller and fuzzy inference for parameter mapping.

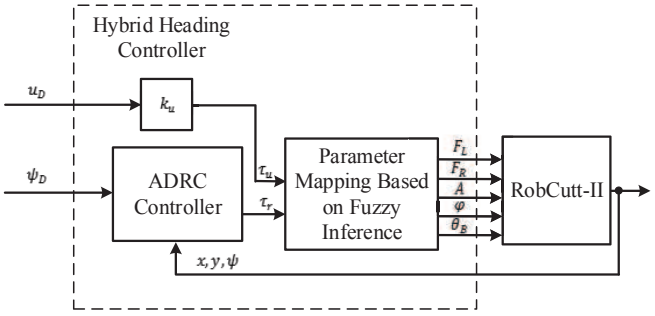

Fig. 5 The control block diagram of hybrid heading control

ADRC can estimate the general disturbances including model uncertainties and external disturbances in real time using an extended state observer (ESO) and then dynamically compensate them in the control signal. For that reason, we employ ADRC controller to output torque τ_r, which forces the RobCutt-II to track the desired heading angle ψ_D based on position and heading feedback.

The characteristic parameter k_u, which reflects the hydraulic resistance, accounts for converting the reference speed u_D to surge force τ_u. Hence the control inputs, namely surge force and yaw torque that two long fins need to generate are calculated. However, the control inputs of RobCutt-II are the parameters of propagating waves on bilateral fins including the left fin frequency, the right fin frequency, amplitude of waves and the phase difference, which are denoted by F_L, F_R, A, φ, θ_B, respectively. Therefore, fuzzy logic model is used to build the nonlinear relationship between force/torque and the parameters of propagating waves. Next, the two components of hybrid heading controller are further described in detail.

ADRC controller

To force the RobCutt-II to track the desired heading angle ψ_D, an ADRC controller is designed in this section. Fig. 6 shows the block diagram of the proposed linear ADRC (LADRC) controller. In particular, tracking differentiator (TD) is used to obtain the differential signal and the tracking signal of the setpoint. An ESO provides an estimate of the internal dynamics of RobCutt-II and the external disturbances which include the environmental disturbances and the unknown measurement error based on control signal τ_r and system outputs ψ in real time. With the dynamic compensation of the estimated information, the system is reduced to a double integrator. Then, a proportional-derivative (PD) controller is sufficient to control it.

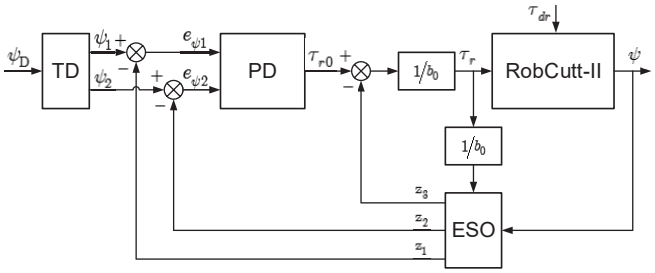

Fig. 6 Block diagram of LADRC controller

Once the observer is designed and well tuned, its outputs z_1, z_2 will track ψ, $\dot{\psi}$ and $z_3 \approx f_r + (b_r - b_0)\tau_r$, where b_0 denotes the estimation of the control gain of Eq. (4). By canceling the effect of f_r using z_3, the ADRC actively compensates for f_r in real time. The ADRC control law for plant Eq. (4) is given by

$$\tau_r = \frac{\tau_{r0} - z_3}{b_{r0}} \tag{5}$$

where $\tau_0 = k_p e_{\psi 1} + k_d e_{\psi 2}$; k_p and k_d are the proportional gain and the derivative gain respectively; $e_{\psi 1} = \psi_1 - z_1$ and $e_{\psi 2} = \psi_2 - z_2$ are states error; ψ_1 is the tracking signal of ψ_D and ψ_2 is the differential signal of ψ_1 subject to the acceleration limit of δ. The linear discrete ADRC controller can be summarized as follows:

$$\begin{cases} \psi_1(k+1) = \psi_1(k) + h\psi_2(k) \\ \psi_2(k+1) = \psi_2(k) + h\,\mathrm{fhan}(\psi_1(k) - \psi_D(k), \psi_2(k), \delta, h_0) \\ e_\psi = z_1(k) - \psi(k) \\ z_1(k+1) = z_1(k) + h[z_2(k) - 3\omega_o e_\psi] \\ z_2(k+1) = z_2(k) + h[z_3(k) - 3\omega_o^2 e_\psi + b_0\tau_r] \\ z_3(k+1) = z_3(k) - h\omega_o^3 e_\psi \\ e_{\psi 1} = \psi_1(k+1) - z_1(k+1) \\ e_{\psi 2} = \psi_2(k+1) - z_2(k+1) \\ \tau_{r0} = k_p e_{\psi 1} + k_d e_{\psi 2} \\ \tau_r = \frac{\tau_{r0} - z_3(k+1)}{b_0} \end{cases} \tag{6}$$

where h is the heading control period; h_0 denotes the filtering factor related to the suppression of noise; ω_o refers to the desired natural frequency of the closed-loop system; k denotes the kth sample constant; fhan is optimal control synthesis function of discrete-time system (Han, 2009).

Parameter mapping based on fuzzy inference

Fuzzy logic model is used to build the nonlinear relationship between the output of ADRC controller and the control input of RobCutt-II. As shown in Fig. 7, the proposed fuzzy approach has two input (i.e., surge force τ_u and yaw torque τ_r) and four output (i.e., the parameters of propagating waves). Fuzzification, fuzzy inference, fuzzy rule base and defuzzification are four main components of the fuzzy model. The universe of discourse of each variable is determined according to the evaluation of previous experiments: $\tau_u \in [-7, 7]$, $\tau_r \in [-5, 5]$, $F_L \in [-40, 40]$, $F_R \in [-40, 40]$, $A \in [10, 40]$, $\varphi \in [0, 120]$. In particular, the sign of fin frequency represents the direction of the propagating waves. The fuzzy sets of τ_u, τ_r, A, φ, F_L, F_R are expressed as T_u, T_r, U_A, U_φ, U_{F_L}, U_{F_R}, respectively. The sets with seven linguistic values for τ_u, τ_r, F_L, F_R are defined: $T_u = T_r = U_{F_L} = U_{F_R} = \{NB, NM, NS, Z, PS, PM, PB\}$; The sets with four linguistic values for A is defined: $U_A = \{PS, PM, PB, PL\}$; The sets with four linguistic values for φ is defined: $U_\varphi = \{Z, PS, PM, PB\}$. Here NB, NM, NS, Z, PS, PM, and PB are linguistic values meaning

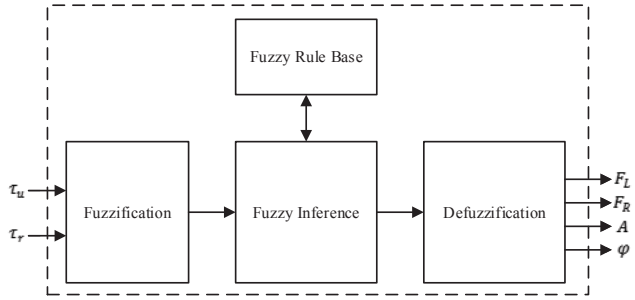

Fig. 7 Block diagram of parameter mapping based on fuzzy inference

negative large, negative median, negative small, zero, positive small, positive median, and positive large, respectively. Thus the standard triangular membership functions utilized are illustrated in Fig. 8.

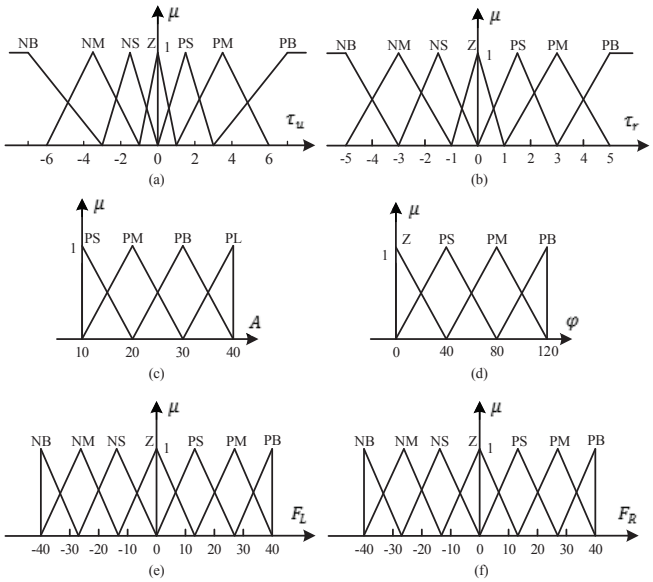

Fig. 8 Membership functions. (a) Membership functions for τ_u. (b) Membership functions for τ_r. (c) Membership functions for A. (d) Membership functions for φ. (e) Membership functions for F_L. (f) Membership functions for F_R.

Table 2 tabulates the specific fuzzy rule base, which is generated on the basis of following two principles: 1) The priority of the heading control is higher than the priority of the surge control. Namely, when yaw torque and surge force are both large, large yaw torque is guaranteed preferentially. 2) When required yaw torque is small while surge force is large, the direction of waves along the two fins should be consistent but the wave frequency should become different to output large surge force and small yaw torque. The max-min inference is used for fuzzy inference and centroid computation is used for defuzzification. Finally, the parameters of propagating waves on bilateral fins are calculated.

EXPERIMENTS

To evaluate the proposed mechanism and control system of the RobCutt-II, two experiments, i.e., course-keeping experiment and course-changing experiment, were performed on the RobCutt-II in an

Table 2 The fuzzy rule base

U_{FL}, U_{FR}, U_A, U_φ		T_r						
		NB	NM	NS	Z	PS	PM	PB
T_u	NB	NB,PB, PL,PB	NB,NS, PB,PB	NB,NM, PB,PB	NB,NB, PB,PB	NM,NB, PB,PB	NS,NB, PB,PB	PB,NB, PL,PB
	NM	NB,PB, PB,PB	NB,NS, PB,PB	NM,NS, PB,PB	NM,NM, PB,PB	NS,NM, PB,PB	NS,NB, PB,PB	PB,NB, PB,PB
	NS	NB,PB, PB,PB	NM,PM, PB,PB	NM,NS, PM,PM	NS,NS, PS,PS	NS,NM, PM,PM	PM,NM, PB,PB	PB,NB, PB,PB
	Z	NB,PB, PB,PB	NM,PM, PM,PM	NS,PS, PS,PS	Z,Z, Z,Z	PS,NS, PS,PS	PM,NM, PM,PM	PB,NB, PB,PB
	PS	NB,PB, PB,PB	NM,PM, PB,PB	PS,PM, PM,PM	PS,PS, PS,PS	PM,PS, PM,PM	PM,NM, PB,PB	PB,NB, PB,PB
	PM	NB,PB, PB,PB	PS,PB, PB,PB	PS,PM, PB,PB	PM,PM, PB,PB	PM,PS, PB,PB	PB,PS, PB,PB	PB,NB, PB,PB
	PB	NB,PB, PL,PB	PS,PB, PB,PB	PM,PB, PB,PB	PB,PB, PB,PB	PB,PM, PB,PB	PB,PS, PB,PB	PB,NB, PL,PB

indoor pool with dimensions of 5m × 4m × 1.1m (length × width × depth). A global visual system connected to console through a USB interface is installed on the pool ceiling. By processing the image information of the RobCutt-II and its surroundings captured by the global visual system, the console can calculate the position and heading information of the RobCutt-II, which are further transmitted to the decision control unit via the UDP protocol in real-time. Next, the output of the decision control unit is sent to the driving unit through the serial ports with a baud rate of 115200 bits/s.

Course-keeping control is to maintain the desired heading angle of the RobCutt-II when it swims forward. In the experiment, the initial heading angle of RobCutt-II was 70° and the desired heading angle was 210°. Moreover, the control period was $0.05s$ and the nominal parameters of ADRC controller were: $\delta = 0.05$, $h_0 = 0.1$, $\omega_o = 5$, $k_p = 9$, $k_d = 6.6$, $b_{\psi 0} = 0.3$. The clip of course-keeping experiment is demonstrated in Fig. 9. Fig. 10 shows the results of ψ, τ_u and τ_r. The control parameters of propagating waves on bilateral fins of the RobCutt-II are illustrated in Fig. 11. It should be noticed that heading changes seem to be accomplished entirely by changing the frequency of the fins. The amplitude of waves and the phase difference are maintained at 30° and 36° respectively, at which the undulatory fin may produce the maximum thrust. The experimental results shows that the proposed hybrid heading controller forced the RobCutt-II to track the reference heading first, which has a settling time of about $12s$ and almost no overshoot. After the heading angle reached the set value, RobCutt-II continued to swim forward with small heading error until the end of the experiment.

Another experiment is the course-changing experiment. In this test, the desired heading was periodically changed after the RobCutt-II entered the current steady state during its movement. The initial heading angle of the RobCutt-II was 7° and the desired heading angle in turn were 10°, 100°, 190°, 280°. Other parameters were consistent with the course-changing experiment. Fig. 12 and Fig. 13 give image sequence and control signals of course-changing experiment, respectively. Fig. 14 shows the control signals of the hybrid heading controller. It is observed that the amplitude of waves is remained at 30° while the phase difference changes over time.

Notice that RobCutt-II firstly changed its heading angle to 10° and then attempted to swim forward holding the desired heading. Then the heading change was changed at $43.3s$ and two more heading changes followed at $78.4s$ and $112.8s$ sequently. Moreover, the actual trajectory matches the commanded trajectory, which shows the effectiveness of the proposed hybrid controller for course-changing control.

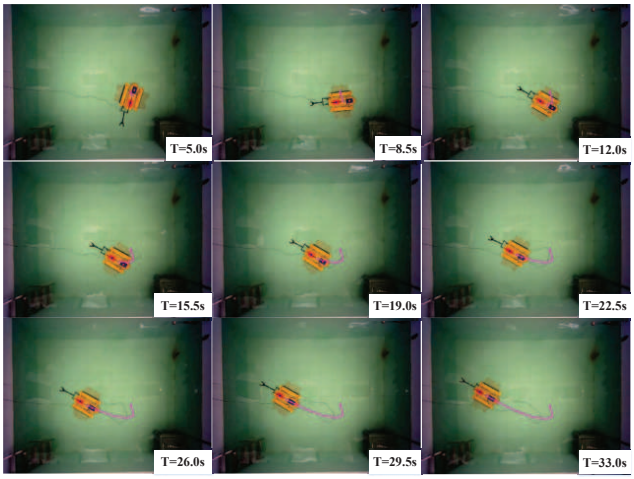

Fig. 9 Image sequence of course-keeping experiment. The pink curve indicates the trajectory of the RobCutt-II.

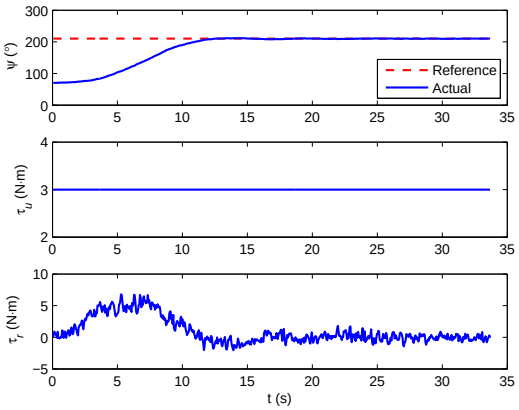

Fig. 10 Experimental results of course-keeping control.

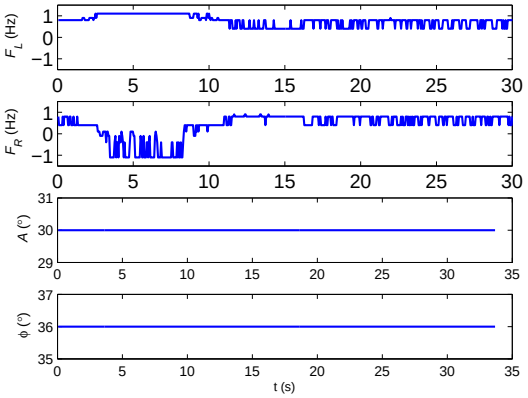

Fig. 11 Control signals of hybrid heading controller in course-keeping experiment.

CONCLUSIONS

A novel BUV named RobCutt-II has been introduced, and its closed loop heading control has been achieved. In the mechanical design, t-

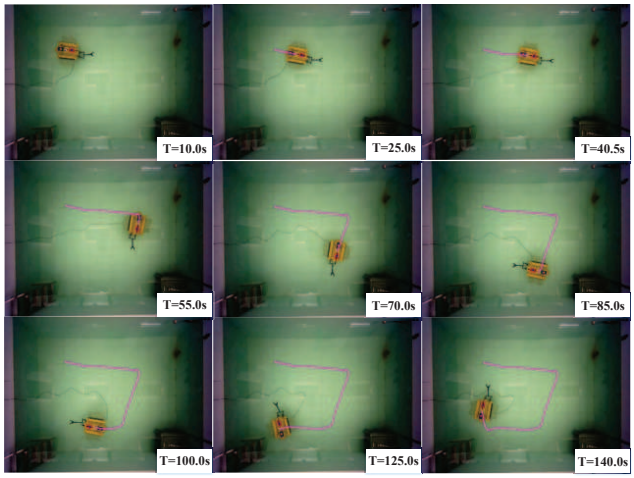

Fig. 12 Image sequence of course-keeping experiment. The pink curve indicates the trajectory of the RobCutt-II.

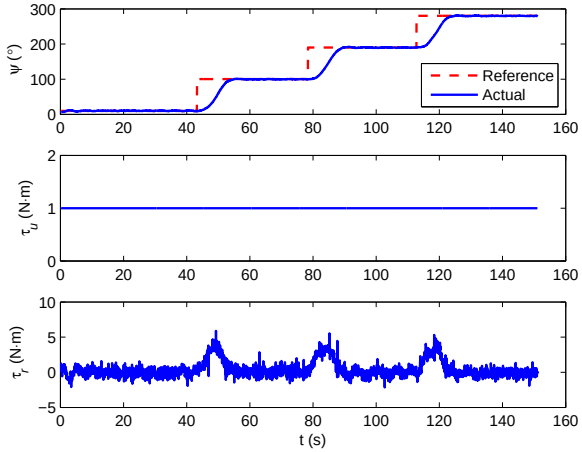

Fig. 13 Experimental results of course-keeping control.

wo biomimetic propulsors with undulatory long fins are installed on both sides of the manipulator system symmetrically. With the coordinated control of the propagating waves on bilateral fins, RobCutt-II can perform many motions, including forward/backward swimming, diving/floating motion, and turning maneuver. In order to realize heading control of the RobCutt-II with model uncertainties, a hybrid control scheme combining ADRC with fuzzy strategy is proposed. The experimental results have demonstrated that the RobCutt-II can achieve accurate heading control by the hybrid controller for underwater missions.

ACKNOWLEDGMENTS

This work was supported in part by the National Key Technology Research and Development Program of China under Grant No.2013BAK03B00, in part by the National Natural Science Foundation of China under Grant 51175496, 61421004, 61333016, and in part by the Beijing Natural Science Foundation under Grant 3141002.

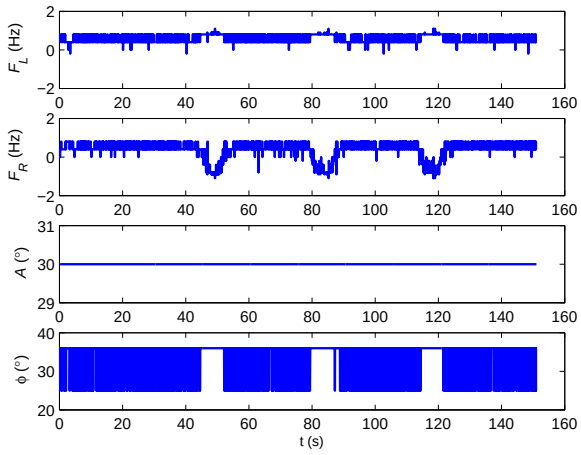

Fig. 14 Control signals of hybrid heading controller in course-keeping experiment.

REFERENCES

Blidberg, DR (2001). "The development of autonomous underwater vehicles (AUV); a brief summary", *Proceedings of the International Conference on Robotics and Automation*, Seoul, Korea.

Chu, WS, Lee, KT, Song, SH, Han, MW, Lee, JY, Kim, HS, Kim, M-S, Park, YJ, Cho, KJ and Ahn, SH (2012). "Review of biomimetic underwater robots using smart actuators", *International Journal of Precision Engineering and Manufacturing*, Vol 13, No 7, pp 1281–1292.

Curet, OM, Patankar, NA, Lauder, GV and MacIver, MA (2011). "Mechanical properties of a bio-inspired robotic knifefish with an undulatory propulsor", *Bioinspiration & Biomimetics*, Vol 6, No 2, p-p 026004.

Fossen, TI (2002). "Marine control systems: guidance, navigation and control of ships, rigs and underwater vehicles", *Marine Cybernetics*.

Han, JQ (2009). "From PID to active disturbance rejection control", *IEEE Transactions on Industrial Electronics*, Vol 56, No 3, pp 900–906.

Hu, T, Low, KH, Shen, LC and Xu, X (2012). "Effective phase tracking for bioinspired undulations of robotic fish models: a learning control approach", *IEEE/ASME Transactions on Mechatronics*, Vol 19, No 1, pp 191–200.

Klir, G and Yuan, B (1995). "Fuzzy sets and fuzzy logic", *New Jersey: Prentice hall*, Vol 4.

Perez, T (2006). "Ship motion control: course keeping and roll stabilisation using rudder and fins", *Springer Science & Business Media*.

Rahman, MM, Sugimori, S, Miki, H, Yamamoto, R, Sanada, Y and Toda, Y (2013). "Braking performance of a biomimetic squid-like underwater robot", *Journal of Bionic Engineering*, Vol 10, No 3, pp 265–273.

Tiaple, Y, Laitongdee, K and Iamraksa, P (2014). "Autonomous underwater vehicle for coastal survey", *Proceedings of the Twenty-fourth International Ocean and Polar Engineering Conference*, International Society of Offshore and Polar Engineers.

Wang, R and Wang, S. (2015). "Design and implementation of a biomimetic underwater propeller with a undulating long fin", *Journal of Huazhong University of Science and Technology (Nature Science Edition)*, Vol 43, No s1, pp 408–411. (in Chinese)

Wang, Y, Wang, S, Wei, QP, Tan, M, Zhou, C and Yu, JZ. (2015). "Development of an underwater manipulator and its free-floating autonomous operation", *IEEE/ASME Transactions on Mechatronics*, No 99.

Wei, QP, Wang, S, Wang, Y, Zhou, C and Tan, M. (2015). "Course and depth control for a biomimetic underwater vehicle - RobCutt-I", *International Journal of Offshore and Polar Engineering*, Vol 25, No 2, pp 81–87.

Yu, Z, Bao, X and Nonami K. (2011). "Course keeping control of an autonomous boat using low cost sensors", *Journal of System Design and Dynamics*, Vol 2, No 1, pp 389–400.

Zhou, CL and Low, KH (2012). "Design and locomotion control of a biomimetic underwater vehicle with fin propulsion", *IEEE/ASME Transactions on Mechatronics*, Vol 17, No 1, pp 25–35.